No evidence of sexual conflict for a novel sperm-derived seminal fluid protein in *Caenorhabditis* nematodes

Short Title: NSPF proteins promote fitness without sexual conflict

Katja R. Kasimatis[1]*, Christine Rehaluk[1], Locke Rowe[1], and Asher D. Cutter[1]*

[1]Department of Ecology and Evolutionary Biology, University of Toronto, Toronto, Ontario, Canada

*Corresponding authors: k.kasimatis@utoronto.ca (KRK) and asher.cutter@utoronto.ca (ADC)

ABSTRACT

Post-insemination molecular interactions involving sperm are an ideal system for linking genotype, phenotype, and fitness. Nematode sperm contain subcellular vesicles known as membranous organelles (MOs) that fuse with the cell membrane upon sperm activation to release their soluble contents into the extracellular space. The second most abundant proteins in the MOs is the conserved Nematode-Specific Peptide family, group F (NSPF) gene family.

We hypothesize that these proteins contribute to seminal fluid upon MO fusion and are part of post-insemination reproductive tract dynamics. We used experimental evolution to compete the wildtype allele against a deletion allele in 10 replicate populations. We calculated a significant mean selective disadvantage of 0.1% for the deletion allele, which indicated that the NSPF genes are an evolutionarily important component of male reproductive success. This conclusion was reinforced by qualitative trends from lower powered single-generation male fertility assays. We then characterized the functional location of NSPF proteins during fertilization using whole-worm immunostaining of a His-tagged *nspf-1* transgene. Throughout male development, we found that NSPF presence and abundance was correlated with reproductive maturity in males, localizing to the seminal vesicle during L4 and to the spicules throughout adulthood. We confirmed that NSPF proteins are transferred to females during mating and hypothesize that proteins adhere to the spicules during transfer. NSPF proteins localize to the vulva and uterus lumen when transferred to mated females and in unmated adult hermaphrodites. These results suggest that the uterine localization of the NSPF proteins is likely a functional property of both male-derived sperm and self-sperm and not simply incidental to the point of transfer during mating. Our study demonstrates that nematodes use a novel mechanism for generating seminal fluid proteins and shows that the highly abundant NSPF proteins likely have a female-beneficial fitness effect.

Keywords: seminal fluid proteins, reproductive fitness, experimental evolution, *Caenorhabditis elegans*

INTRODUCTION

To understand the extent of adaptive evolution, we must link a phenotype with its underlying genetic basis and effect on fitness (Barrett & Hoekstra, 2011). By connecting the layers of the genotype-phenotype-fitness map we gain insight on the mechanisms that drive adaptation (Lewontin, 1974). Understanding these linkages will often demand an integrated, interdisciplinary experimental approach, which is necessarily challenging. Post-insemination reproductive interactions, however, offer an ideal stage of the lifecycle for mapping these relationships because their impact on reproductive fitness is direct, such that an adaptive advantage of one variant over another should lead to an increase in reproductive success. Additionally, the interactions involving cells, proteins, and small molecules simplifies the mapping of their genetic basis (McDonough *et al.*, 2016). Despite these direct and simplified linkages, connecting reproductive genes with a clear, consistent phenotype and a reproducible, quantifiable effect on fitness has proved challenging.

Post-insemination reproduction studies have largely focused on interactions mediated by seminal fluid. Seminal fluid is a complex mixture of cells, proteins, and other small molecules that are transferred to the female along with sperm (Poiani, 2006; Perry *et al.*, 2013). As a whole, seminal fluid is critical for male fertility – sperm alone is not enough to ensure fertilization – and is implicated in complex behaviors, such as sperm competition, male-female signaling and conflict (Poiani, 2006). Most functional work on these seminal fluid proteins comes from the study of dozens of *Drosophila* accessory gland proteins (Acps) (Chapman, 2011). The genes underlying many of these Acps are characterized by their elevated evolutionary rate relative to non-reproductive proteins, indicating adaptive evolution (Begun *et al.*, 2000; Swanson & Vacquier, 2002; Clark *et al.*, 2006; Wilburn & Swanson, 2016). The complexity of seminal fluid proteins coupled with their rapid evolution and some evidence of harmful effects on females have led to the paradigm that these proteins are beneficial to male fitness but detrimental female fitness (Sirot *et al.*, 2015). Perhaps the best studied Acp, Sex Peptide, has become a textbook example of post-insemination sexual conflict (Arnqvist & Rowe, 2005; Hopkins & Perry, 2022). However, this protein does not always fit the conflict paradigm it has come to represent (Hopkins & Perry, 2022). In particular, molecular evolution analysis of Sex Peptide indicates molecular constraint, which is not consistent with evolution driven by sexual conflict (Cirera & Aguade, 1997). Additionally, when individual components of fitness have been quantified, environmental

factors appear to impact when Sex Peptide is detrimental or even beneficial to female fitness (Hopkins & Perry, 2022). These deeper analyses along with similar studies on other Acps (Wong & Rundle, 2013) suggest that seminal fluid evolution is more nuanced than the sexual conflict narrative alone and indicate that employing new approaches and new taxa may provide a more precise and complete understanding of the complex roles and fitness effects of seminal fluid proteins.

Caenorhabditis nematodes are powerful model system for integrating across the layers of the genotype-phenotype-fitness landscape and are ideal for expanding our view on the extent of evolution by sexual conflict and discovering new roles for seminal fluid proteins. First, mating system differs across the genus, with *C. elegans* representing a lineage transition from obligate outcrossing to hermaphroditic self-fertilization (Baldi *et al.*, 2009). Using the genetic tools developed in *C. elegans*, researchers can manipulate hermaphrodites to develop as pseudo-females that rely on males to reproduce, which allows direct comparison of the genetics and fitness effects between self-sperm and male-derived sperm to disentangle conflict and cooperation. Additionally, broader contrasts can be made among closely related species with different mating systems and therefore varying opportunities for sexual conflict (Ting *et al.*, 2014; Yin *et al.*, 2018). Second, the small size and rapid generation time of nematodes make them amenable to fitness assays within and across multiple generations. Multi-generation assays allow for detection and quantification of even small fitness effects. Finally, nematodes have unique amoeboid-like crawling sperm which can be visualized through the transparent cuticle, allowing for spectacular live visualization of sperm and seminal fluid dynamics inside of females or hermaphrodites (Smith & Stanfield, 2011; Ting *et al.*, 2014; Hansen *et al.*, 2015; Yin *et al.*, 2018). Very few seminal fluid proteins, however, have been identified and functionally examined in *Caenorhabditis* (Smith & Stanfield, 2011; Yin *et al.*, 2018). Thus, this system provides an underexploited opportunity for discovering new features of reproductive evolution that can be evaluated and, perhaps, challenge existing paradigms.

An intriguing component of nematode sperm cells are subcellular vesicles known as membranous organelles (MOs). In inactive spermatids, MOs are located around the periphery of the cell (Ellis & Stanfield, 2014). Upon ejaculation, spermatids are released from the seminal vesicle and undergo activation as they pass through the vas deferens. During activation, MOs fuse with the cell membrane and create cup-like structures as well as releasing their soluble

102 protein contents into the extracellular space (Ellis & Stanfield, 2014). No accessory gland-like
103 tissues have been identified in *Caenorhabditis* and the source – as well as contents – of seminal
104 fluid are unknown. Consequently, we hypothesize that these MO fusions provide a novel
105 contribution to the seminal fluid proteome. Characterization of the MO proteome identified the
106 Nematode-Specific Peptide family, group F (NSPF) as the second most abundant set of proteins
107 in the MO (Kasimatis *et al.*, 2018). Kasimatis *et al.* (2018) additionally showed that the NSPF
108 genes are conserved in both sequence identity and synteny across the genus. Transcriptomic data
109 support the molecular evolution analyses by capturing NSPF expression in *C. elegans* males
110 along with NSPF ortholog expression in *C. remanei* males (Albritton *et al.*, 2014). Interestingly,
111 transcriptomic data also identify expression in *C. elegans* hermaphrodites but not *C. briggsae*
112 hermaphrodites, suggesting that this gene family has been conserved in at least some self-sperm
113 pathways (Albritton *et al.*, 2014).
114 Here we investigate the function of the NSPF gene family in fertilization by
115 interconnecting the layers of the genotype-phenotype-fitness landscape. We estimate the
116 contribution of the NSPF genes to female reproductive fitness using a combination of within
117 generation fertility assays and 20 generations of experimental evolution. We then use
118 immunostaining to identify the functional regions that NSPF proteins are associated with in
119 males and females/hermaphrodites. Our results indicate that the NSPF proteins are a component
120 of seminal fluid with a net fitness benefit and imply that even a highly abundant seminal fluid
121 protein can have a subtle function.
122

123 **MATERIALS AND METHODS**

124 **Molecular biology**

125 To create a tagged *nspf-1* gene, guides targeting the sequence in the same intergenic region
126 utilized by the ttTi5650 MosSCI site have previously been described (Dickinson *et al.*, 2015) and
127 inserted into pDD162 (Addgene #47549) to make plasmid pMS4. The repair template plasmid
128 (pKK4) was assembled using the NEBuild HiFi Kit (NEB) from a combination of a restriction
129 digest fragment and a synthetic gBlock Gene Fragment (IDT). The gBlock included the 647 base
130 pairs upstream of *nspf-1* as the promoter region, the *nspf-1* coding sequence with six histidines
131 added before the stop codon, and the *tbb-2* 3' UTR. The plasmid was purified using the GeneJET

132 Plasmid Miniprep Kit (Thermo Scientific) and assembly junctions were verified by Sanger
133 sequencing. A complete list of primers can be found in Table S1.

134 **Strain generation**

135 All strains used in this study are listed in Table S2. The NSPF genes were previously deleted
136 using CRISPR/Cas9 to create strain PX814 (fxDf1 (II: 2,484,339 - 2,487,244)) (Kasimatis *et al.*,
137 2018). To generate an obligate outcrossing deletion strain, JK574 (*fog-2*(q71) V) was crossed
138 with PX814 and then backcrossed 5 times with JK574 to create the obligate outcrossing, deletion
139 strain VX194. The deletion region was verified by Sanger sequencing.

140 Insertion of the His-tagged *nspf-1* transgene was done by CRISPR/Cas9 using standard
141 methods (Dickinson *et al.*, 2015). Briefly, a mixture of 10ng/µL repair template plasmid,
142 50ng/µL plasmid encoding CAS9 and the guide RNA, and 2.5ng/µL of the co-injection plasmid
143 pZCS16 was injected into the gonad of young adult hermaphrodites from PX814. Hygromycin B
144 (BioShop) was added to the injection plates at a final concentration of 250µg/mL three days after
145 injection and hygromycin resistance (HygR) was used as a selectable event. Worms were kept at
146 25ºC for the first five days immediately following injections and then transferred for 20ºC for
147 subsequent generations. Successful insertion was confirmed by PCR (Table S1) and Sanger
148 sequencing. Worms were then backcrossed five times to PX814 to create the final strain VX300
149 (yf*Si*1[*nspf-1*p::*nspf-1*::6xHis::*tbb-2* 3' UTR + loxP, II:8420157]). We tagged the C-terminal of
150 *nspf-1* since these proteins are predicted signaling peptides (Kasimatis *et al.*, 2018) and, thus, the
151 C-terminal is likely included in the mature peptide.

152 **Fertility Assays**

153 We assayed the overall reproductive success of VX194 deletion males late in adulthood. We
154 isolated virgin deletion males on day 1 of adulthood. On day 5 adulthood, single males were
155 mated with three wildtype, virgin females (strain JK574) for 24 hours. As a control, wildtype
156 males (strain JK574) were mated to wildtype females following the same timing and male to
157 female ratio. Matings were conducted on small NGM-agar plates (35 mm diameter) seeded with
158 10µL OP50 *Escherichia coli*. After 24 hours, each male was removed and the females were
159 transferred to a new small plate to continue laying eggs. Females were transferred to new plates
160 every 24 hours until progeny production ceased. The total number of progeny was counted as a
161 measure of each male's reproductive success (File S1). Fertility data were analyzed using R (R

162 Core Team, 2020), with the significance of non-competitive reproductive success evaluated
163 using Welch's Two Sample t-test and an analysis of the power of the comparison computed.
164 Previous fecundity data were replotted using the data available in Kasimatis et al. (2018)
165 Additional File 9.

166 **Experimental evolution design and worm culture**

167 To create a base population, reciprocal crosses of virgin females and males from strains JK574
168 and VX194 were performed. The F1 heterozygous progeny were divided into 10 replicate
169 populations of 500 worms with equal numbers of each sex to start the first generation. After
170 generation one, populations were expanded to a census size of N = 1,000 worms per replicate
171 and evolved for 20 generations. To start each generation, age synchronized larval stage 1 (L1)
172 worms were plated onto four 10 cm NGM-agar plates seeded with OP50 *E. coli* at 20ºC with a
173 density of 250 worms per plate (Brenner, 1974; Kenyon *et al.*, 1993). Worms were left to mate
174 for the first five days of adulthood before eggs were once again collected on day six to
175 synchronize for the next generation. During this mating time, worms within each replicate were
176 pooled and redistributed to fresh NGM-agar plates twice to ensure they never starved. A subset
177 of worms from all replicates was frozen every five generations for future experiments. At
178 generation eight all worms were frozen and the experiment paused for five months due to
179 COVID-19 lockdown restrictions.

180 **Amplicon sequencing and read calling**

181 We performed amplicon sequencing on pooled samples of 500-800 L1 worms from experimental
182 evolution generations 11 and 20. Two control samples were generated, each with approximately
183 700 worms: 1) F1 heterozygous progeny generated by crossing strains JK574 and VX194, and 2)
184 pooled worms generated by mixing an equal number of JK574 and VX194 worms and sampling
185 from this pool. The wildtype allele was amplified using forward primer (5' to 3')
186 TGCAATGGATTTCTGGTGATAAC and reverse primer (5' to 3')
187 TCTGGCAGTAGGAAAGTGAG, yielding a product of size 230 base pairs. The deletion allele
188 was amplified using forward primer (5' to 3') AGGATAAGAGAGACCCAGAC and reverse
189 primer (5' to 3') TCTGGCAGTAGGAAAGTGAG, yielding a product of size 275 base pairs.
190 PCR products were generated using the OneTaq Quick-Load 2x PCR Master Mix with Standard
191 Buffer (NEB) in accordance with manufacturer instructions with *C. elegans* genomic DNA. PCR

192 products were purified using QIAquick PCR Purification kit (Qiagen) and normalized to
193 20ng/uL. Products were sequenced using GENEWIZ Amplicon-EZ services.
194 Reads for each sample were filtered using bioawk (https://github.com/lh3/bioawk) to
195 exclude reads <50 base pairs in length and with a mean quality score <30. Reads in each sample
196 >230 base pairs in length were then blasted to the deletion reference sequence and retained if the
197 blast score was significant. All remaining reads were then blasted to the unique reference
198 sequence for both the wildtype (bases 1-102) and deletion (bases 1-147) alleles. A read was
199 called as a wildtype or deletion allele based on the best E-value and bit score (File S2). Final
200 counts ranged from 89,721 to 132,685 reads per sample.

201 **Estimating selection**

202 Read data were analyzed using the R statistical language v4.0.0 (R Core Team, 2020). Read
203 counts across all time points were fit using a generalized linear mixed model with a binomial
204 logistic distribution: glm((WT_{count}, DEL_{count}) ~ time). We fit two different linear models to
205 account for biases during PCR amplification as suggested by the frequency of each allele in the
206 control samples (i.e., 73% wildtype and 27% deletion). Model 1 assumed the frequency of each
207 allele to be 50% (i.e., 500 copies of the wildtype allele and 500 copies of the deletion allele for a
208 heterozygous population of N = 500), since all worms were heterozygous at the start of the
209 experiment. Model 2 used only the allele frequencies estimated from the amplicon sequencing at
210 generations 11 and 20. While we report the results of both models, Model 2 provides a better fit
211 ($AIC_{Model\ 1}$ = 146,842; $AIC_{Model\ 2}$ = 146,670) and represents a more conservative estimate of
212 selection.
213 The neutral expectation was determined by simulating in R allele frequency dynamics at
214 a single locus in a population subject to genetic drift and random mating. We simulated 100
215 populations of 1,000 individuals. In the first generation, all individuals were heterozygotes. The
216 genotype frequencies of females and males were multiplied to give a matrix of the relative
217 frequencies of the possible random mating pairs. Mating pairs were then randomly sampled from
218 this distribution to generate offspring to start the next generation.

219 **Whole-worm immunohistochemistry**

220 Worms were formaldehyde-fixed and stained following a modified version of the Ruvkun and
221 Finney protocol (WormAtlas). Briefly, worms were cultured at 20ºC on 10cm NGM-agar plates
222 containing 100ng/mL carbenicillin and seeded with formaldehyde killed *E. coli* OP50 (following

223 Rogers *et al.*, 2006). At each developmental stage used, populations of at least 1,000 worms were
224 fixed in a 1% formaldehyde solution and flash frozen in dry ice with ethanol. Incorrect antibody
225 binding was blocked using solution of: 0.3M glycine, 10mM imidazole, 1% BSA, 0.5% skim
226 milk, and 0.25% Triton-X-100 in PBS. Worms were stained for 1 hour at room temperature
227 using a 1/4000 dilution of Recombinant Alex Fluor 488 Anti-6x His Tag antibody (Abcam
228 #ab237336) and co-stained with DAPI. The complete method along with buffer recipes can be
229 found in File S3.

230 To examine the localization of *nspf-1* in males and hermaphrodites across development,
231 VX300 male-rich populations (~40% males) were age synchronized by bleaching
232 {Kenyon:1988uc} and then formaldehyde-fixed during: L3 (28 hours post-L1), L4 (40 hours
233 post-L1), day 1 of adulthood (46 hours post-L1), day 2 of adulthood (70 hours post- L1), and day
234 8 of adulthood (190 hours post-L1). As a control, JK574 males and pseudo-females were
235 concurrently cultured and fixed at the same developmental stages. In our hands, worms
236 developed more slowly and less synchronously on plates with dead OP50 than on live OP50.
237 Thus, the exact time in development may be asynchronous between worms, but the
238 developmental stages were accurate. At least 100 stained worms from each strain × sex ×
239 developmental stage were scored for the presence and location of fluorescence (File S4). The
240 localization of fluorescence was characterized as occurring in one or more of the following
241 regions: head, distal gonad, proximal gonad (including the spermathecae or seminal vesicle),
242 uterus/vas deferens, vulva/cloaca, or tail. Worms were categorized as "not stained" if no
243 fluorescence was observed.

244 To determine whether or not males transfer NSPF-1 to females during mating, we crossed
245 JK574 pseudo-females with VX300 males. Both strains were age-synchronized by bleaching
246 followed by isolation of virgin pseudo-females (n = 400) and males (n = 150) during late L4 to
247 10cm NGM-agar plates containing 100ng/mL carbenicillin and seeded with formaldehyde-killed
248 *E. coli* OP50 (n = 3 replicate plates). Worms were mated overnight and then formaldehyde-fixed
249 and stained. One hundred pseudo-females were scored for the presence and location of
250 fluorescence.

251 Count data for the presence of fluorescence were analyzed using a χ^2 test based on a
252 contingency table of strain × presence of fluorescence for each sex and developmental stage
253 separately. Specifically, we tested the null hypothesis of no difference between counts of stained

254 individuals and counts of unstained individuals between the control (JK574) and His-tagged
255 (VX300) strains. All analyses were conducted in R (Team", 2020).

256 **Dissected gonad immunohistochemistry**

257 Testes were methanol-fixed and stained following a modified version of the Shakes *et al.* (2009)
258 protocol. Briefly, worms were cultured at 20ºC on 10cm NGM-agar plates and seeded with *E.*
259 *coli* OP50. Young adult males were decapitated using a 30 gauge needle to release the gonad and
260 then transferred to ColorFrost Plus slides (Fisher Scientific). Gonads were fixed in methanol
261 followed by acetone. Incorrect antibody binding was blocked using solution of: 0.3M glycine,
262 10mM imidazole, 1% BSA, and 0.25% Triton-X-100 in PBS. Worms were stained for 1 hour at
263 room temperature using a 1/4000 dilution of Recombinant Alex Fluor 488 Anti-6x His Tag
264 antibody (Abcam #ab237336) and co-stained with DAPI. The complete method along with
265 buffer recipes can be found in File S3. Image stacks were processed using ImageJ.
266

267 **RESULTS**

268 **Deletion of the NSPF genes decreases male fitness**

269 Previous experiments on young adult male fertility showed no significant difference in total
270 fecundity between wildtype males and males with all three copies of the NSPF genes deleted
271 (i.e., deletion allele) (Fig. S1A) (Kasimatis *et al.*, 2018). Using old males (day 5 of adulthood),
272 we repeated these non-competitive, total fecundity assays to determine whether NSPF proteins
273 improved male sperm fertilization ability in a phase of the life cycle when male fertility is
274 declining overall. Although the mean fecundity of old males with the deletion allele trended
275 lower than wildtype males (x_{del} = 459; x_{wt} = 481.9), the effect was not significant (p = 0.85; Fig.
276 S1A). This nominal decrease in fecundity of males with the deletion allele was similar to what
277 was previously seen with young adult males under a competitive male setting, suggesting that
278 NSPF function is potentially age-independent (Kasimatis *et al.*, 2018; Fig. S1B). However, given
279 the experiment size and high reproductive variance, a difference between genotypes of 71%
280 would be required to achieve 80% power to detect a significant difference. Thus, within-
281 generation assays likely are not sufficiently sensitive to capture the nuanced fitness effects
282 suggested by the trend means, despite the high abundance of these proteins.

283 We turned to experimental evolution to overcome these power limitations of within-
284 generation experimental design. Specifically, we competed the wildtype allele against the

285 deletion allele in an obligate outcrossing *C. elegans* population by evolving ten replicate
286 populations of 1,000 individuals from a base population that was heterozygous at the NSPF locus
287 in an otherwise homogeneous genetic background. After 20 generations, we documented a
288 significant overall decrease in the frequency of the deletion allele across replicates (Model 1: z-
289 value = 3.3, p = 0.001; Model 2: z-value = 2.3, p = 0.02). Additionally, the change in frequency
290 exceeded that expected by neutral processes alone in seven of the ten replicates (Fig. 1). These
291 results support the within generation fecundity trends and indicate a direct net fitness cost when
292 the NSPF genes are removed, such that the wildtype allele confers an approximately 0.1% fitness
293 advantage over the deletion allele (Model 1: s = 0.001; Model 2: s = 0.0008). Together, the
294 favoring of the wildtype allele coupled with the fecundity do not provide evidence of a cost of
295 the NSPF proteins during mating. Rather, they provide a net fitness effect that is congruent with
296 being beneficial to at least one sex.

297 **NSPF proteins localize to the spicules in adult males**

298 We characterized the functional location of NSPF proteins during fertilization using whole-worm
299 immunostaining of a His-tagged *nspf-1* transgene re-inserted into the deletion allele background
300 (PX814). We scored the presence the fluorescent antibody bound to NSPF-1::6xHis in six
301 anatomical regions: head, distal gonad, proximal gonad, vas deferens, cloaca, and tail (Fig. 2A).
302 Throughout male development, we found that NSPF presence and abundance was correlated
303 with male reproductive maturity (Fig. 2B; Fig S2). During larval stage 3 (L3), the gonad is still
304 developing and no staining was present, which supports our previous finding that NSPF
305 production is linked with sperm production (File S4). Sperm production begins during the L4
306 stage and correspondingly L4 males had staining in both the distal (n = 17 of 126) and proximal
307 gonad (n = 1 of 126; Fig. 3A). Interestingly, 43% of L4 males had staining in the tail region (n =
308 55 of 126) specifically overlapping with the developing spicules. These patterns are significantly
309 different from control males (χ^2 = 175.5, df = 3, p < 0.0001), of which only one individual
310 showed non-specific staining along the cuticle in the proximal gonad region (Fig. 3B).

311 In adult males, NSPF proteins localized solely to the spicules (Fig. 3C). Abundance
312 appeared highest on days 1 and 2 of adulthood with 100% of males (n = 100 and 150,
313 respectively) showing staining in the tail region (Fig. 2B). Again, these patterns were
314 significantly different from the off-target staining or spicule auto-fluorescence observed in
315 control males during day 1 (n = 13 of 99 stained; χ^2 = 149.5, df = 1, p < 0.0001) and day 2 (n =

316 45 of 150 stained; $\chi^2 = 158.5$, df = 1, $p < 0.0001$) of adulthood (Fig. 3D). Older males, however,
317 had a decreased signal of NSPF proteins (n = 59 of 106), though still significantly different from
318 control males ($\chi^2 = 39.4$, df = 1, $p < 0.0001$). This pattern of protein abundance throughout
319 development suggests that NSPF production is tightly correlated with spermatogenesis and peak
320 reproductive output and mating activity during early adulthood.
321 While immunostaining of whole adult worms did not identify NSPF protein within the
322 gonad, dissected testes of adult males confirmed localization of NSPF within spermatids (Fig.
323 S3). The punctate patterning around the nucleus overlaps with the location of MOs, which
324 supports the proteomic characterization of this gene family. Thus, whole worm immunostaining
325 likely lacked the sensitivity to visualize staining within small sperm subcellular structures.

326 **Males transfer NSPF proteins to the female uterus during mating**

327 To test our hypothesis that NSPF proteins form a constituent of seminal fluid, we examined
328 whether males transferred NSPF proteins during mating. Specifically, control pseudo-females
329 (JK574) were mated with His-tagged males (VX300) for 24 hours. Of the pseudo-females
330 without eggs in utero, 38% (n = 8 of 21) had a clear signal of staining around the vulva and in the
331 uterine space (Fig. 4A). This signal was significantly different from that of control females
332 mated to control males ($\chi^2 = 9.7$, df = 2, p = 0.008; Fig. 4B). Only 12% (n = 15 of 129) of
333 pseudo-females with eggs in utero showed a clear signal of staining, which was not significantly
334 different from pseudo-females mated to control males ($\chi^2 = 0.53$, df = 1, p = 0.47). However, in
335 these females the NSPF proteins appear to be in the uterus lumen, which suggests that eggs may
336 mask the fluorescent signal (Fig. 4C). These results indicate that males transfer NSPF proteins
337 during ejaculation and support our hypothesis that MOs contribute proteins to seminal fluid.

338 **NSPF proteins localize to the uterus of unmated hermaphrodites**

339 To determine if self-sperm NSPF patterns differed from male-derived sperm patterns, we
340 characterized NSPF localization in His-tagged hermaphrodites (VX300) raised in the presence of
341 males throughout development. Again, L3 individuals showed no signal of staining (File S4). L4
342 hermaphrodites, however, had little to no staining and did not significantly differ from control
343 females (p = 1; Fig. 2C) despite mRNA expression of *nspf-1* during this developmental stage
344 (Harris *et al.*, 2019). The non-overlapping mRNA and protein localization patterns are likely to
345 be an artifact of our whole-animal immunostaining procedure. Adult hermaphrodites all showed

346 the same vulva and uterus localization pattern of staining as we observed in mated, control
347 females (Fig. 2C; Fig. S2). On days 1 and 2 of adulthood 54% (n = 54 of 100) and 41% (n = 61
348 of 150) of hermaphrodites, respectively, showed staining, which was significantly more than
349 control females (Day 1: $\chi^2 = 49.9$, df = 1, $p < 0.0001$; Day 2: $\chi^2 = 22.6$, df = 1, $p < 0.0001$). On
350 day 8 of adulthood, 67% (n = 90 of 134) of hermaphrodites showed the same significant staining
351 pattern ($\chi^2 = 147.2$, df = 6, $p < 0.0001$; Fig. 2C). Because self-sperm are depleted by day 8 late in
352 adulthood (Hirsh *et al.*, 1976), these data further support the male transfer of NSPF proteins to
353 the uterus. Across all developmental time points, there was an unexpected absence of signal in
354 the spermathecae, likely due to experimental constraints.
355 To distinguish whether the early adulthood signal of NSPF staining was caused by self-
356 fertilization or mating, we examined a male-less population of His-tagged hermaphrodites on day
357 1 of adulthood prior to the start of egg laying. If the NSPF proteins were costly to female
358 reproduction, then we would expect self-sperm derived NSPF to be lost or significantly reduced.
359 We found that 59% (n = 59 of 100) of hermaphrodites showed the same vulva and uterus pattern
360 of staining (Fig. 4D) despite no opportunity for male transfer of NSPF proteins. This frequency
361 was not significantly different from the number of day 1 hermaphrodites raised in the presence of
362 males ($p = 0.57$). These results suggest that the uterine localization of the NSPF proteins –
363 whether secreted by self-sperm or male sperm – likely reflects their site of activity and not
364 simply a byproduct of the point of transfer during mating. Moreover, they reinforce the benefit of
365 NSPF proteins to reproductive fitness and imply that this benefit is directed toward female
366 reproduction.
367
368 **DISCUSSION**
369 Seminal fluid is a complex bioactive mixture whose components are implicated in a variety of
370 reproductive, behavioral and physiological functions and thus likely evolves under multiple
371 selective pressures. By linking the genes creating seminal fluid proteins with their evolutionary
372 history, effect on fitness, and phenotypic contribution we can understand the evolutionary forces
373 driving seminal fluid evolution through its impacts on reproductive function. We took an
374 integrative approach to connect the highly abundant MO NSPF proteins across the genotype,
375 phenotype, fitness landscape. We confirmed that the NSPF genes are indeed a component of
376 seminal fluid that is transferred to females, which demonstrates that MO fusion provides a novel

377 source of seminal fluid proteins. Moreover, the localization of NSPF proteins differ from that of
378 mRNA transcripts, highlighting the nested layers between genotype space and phenotype space
379 that can often be overlooked. Finally, we quantified the small, but significant contribution made
380 to reproductive fitness by the presence of NSPF proteins, suggestive of a fitness benefit
381 potentially to females. Together this work demonstrates the power of *Caenorhabditis* to
382 disentangle beneficial versus antagonistic effects of seminal fluid proteins and expand our
383 perspective of seminal fluid protein function.

384 The manipulable hermaphroditic mating system of *C. elegans*, relative to study systems
385 like *Drosophila*, offers a novel means of distinguishing sexual conflict from sexual cooperation
386 between male-derived sperm and self-sperm interactions (Schärer *et al.*, 2015). We capitalized
387 on this advantage to show that NSPF production is not only retained during the lineage transition
388 to self-fertilization, but that the proteins localize to the same uterus region in unmated
389 hermaphrodites as mated females (Fig. 4). This pattern supports the conserved molecular
390 evolution of the *nspf* gene sequences and implies that the function of the sperm-dependent NSPF
391 proteins within the uterus is mating-independent. Importantly, the conserved expression in
392 hermaphrodites indicates that these proteins are not involved in sexual conflict, as there would be
393 strong selection favoring their loss (Yin *et al.*, 2018). Instead, these genes appear beneficial to
394 fitness in a female-biased manner, as supported by fitness assays. In particular, if NSPF genes
395 provided an advantage to males to the detriment of females, we would expect females mated
396 with deletion males to trend toward higher reproductive success than females mated with
397 wildtype males. However, our assay and previous assays support the opposite of such a scenario,
398 suggesting NSPF promotes sexually-concordant reproductive fitness, as shown more
399 convincingly during experimental evolution.

400 A common challenge in evolutionary biology is to detect the fitness effects of variants at
401 a single gene (Barrett & Hoekstra, 2011). Our experimental evolution design to compete the
402 wildtype and deletion alleles in a highly-replicated fashion allowed us to compound small effect
403 sizes over tens of generations. The nematode model system allows for this approach to be done
404 at a larger scale and over a longer time periods than similar studies (Wong & Rundle, 2013),
405 which, when coupled with genomics, provides greater power to detect small or fluctuating
406 selection coefficients. The overall trend across replicates was a decrease in the frequency of the
407 deletion allele beyond the neutral expectation (Fig. 2). The estimated selection coefficient,

408 despite being small, would be powerful enough to prevent *nspf* gene loss over time in nature. The
409 frequency of the deletion allele did not continually decrease in every replicate at each sampling
410 time point, however, which likely reflected a combination of variance and stochasticity during
411 mating along with sampling error and the relatively small selection coefficient. The fluctuation
412 of the deletion allele could also reflect the environment conditions in the lab which do not
413 perfectly replicate nature, where the NSPF proteins may provide a greater or more consistent
414 benefit in populations with larger effective sizes. This approach of allelic competition in
415 experimental evolution (Gray & Cutter, 2014; Teotonio *et al.*, 2017) may represent a promising
416 avenue for future seminal fluid protein studies, and for genetic variants of other phenotypes,
417 where small fitness effect sizes have proved challenging to characterize.

418 The localization of NSPF protein to the spicule (Fig. 3) and uterus (Fig. 4) was
419 unexpected given that the NSPFs were previously characterized as being associated with sperm
420 MOs (Kasimatis *et al.*, 2018) and that mRNA expression data indicated that all three *nspf* genes
421 are expressed in the gonad only (Kruse *et al.*, 2016). Staining of dissected testes provided the
422 necessary sensitivity to confirm that NSPF proteins localize to spermatid MOs. Our whole-worm
423 staining approach did, however, identify additional regions of localization that may result from
424 the anatomical difference in the location of inactivated versus activated sperm. The activation
425 process occurs as sperm pass from a male to a female/hermaphrodite while the spicules are
426 everted in the vulva, thus creating a direct link between MO fusion and the spicules. This overlap
427 in timing, however, does not explain the spicule signal seen in L4 males, which warrants further
428 work. In hermaphrodites, the parsimonious hypothesis is that NSPF proteins passively diffuse
429 from the spermathecae, where activated sperm reside, to the uterus. The location of NSPF
430 proteins within the uterus is similar to other proteins that males transfer, which originate in
431 newly identified extracellular vesicles (Nikonorova *et al.*, 2022). While the NSPFs do not appear
432 in these vesicles, it is possible that this alternative vesicle type also contributes to seminal fluid
433 proteins, supporting our finding that nematodes employ a distinct mechanism for secreting
434 seminal fluid proteins than either mammals or *Drosophila* (McGraw *et al.*, 2015).

435 Our data motivate multiple hypotheses for future testing to narrow down the specific
436 beneficial function of the NSPF proteins. First, the NSPF proteins could interact with a male-
437 female signaling network that promotes egg laying. While the interacting partner for NSPF
438 proteins remains unknown, it is possible that NSPFs bind to muscle proteins that form the uterus

walls and are involved in egg laying behavior. Under this hypothesis, localization to the spicules is puzzling. However, previous work has shown the females pressurize the gonad to push some of the ejaculate mass and spicules out of the vulva (Barker, 1994; Kleemann & Basolo, 2007). This process could create a residue on the spicule cuticle as a byproduct, though we cannot rule out a functional relationship between the NSPF proteins and spicule cuticle.

Alternatively, the NSPF proteins could impact the uterine environment. Specifically, seminal fluid of some species contains anti-microbial factors (Samakovlis *et al.*, 1991; Gao & Zhu, 2016). Given the density of protein right above the vulva, one hypothesis is that the NSPF proteins play an anti-microbial role to protect the uterus from bacterial infection. Previous work has shown that the uterus is exposed to pathogenic infection from the external environment during mating and egg laying (Muir & Tan, 2008). The male spicules are presumably also exposed during eversion, and thus any anti-microbial activity of the NSPF residue on the spicules might serve to prevent bacterial infection when the spicules retract. Biochemically, the alpha-helix structure of NSPF proteins lends plausibility to this hypothesis, as such secondary structures can confer generic bacterial lysing properties (Huan *et al.*, 2020). Future work testing the fitness effects of the NSPF deletion allele in worms raised in more pathogenic bacteria is warranted.

Our work demonstrates the complex but subtle dynamics of seminal fluid proteins uncovered when using integrative approaches. The NSPF seminal fluid proteins, in particular, exhibit sexually-concordant rather than sexually-antagonistic fitness effects. We also showed how *Caenorhabditis* nematodes are an excellent system for expanding our knowledge of post-insemination interactions not only for their technical benefits, but also for their novel sperm components and potential for making mating system contrasts. Connecting the layers of the genotype-phenotype-fitness map for seminal fluid proteins will help us uncover the genetics of fertility and the evolution of reproductive success.

Acknowledgements: We thank the Phillips lab for sharing plasmids pMS4 and pZCS16 and strain PX814. We thank Zachary Stevenson for transgenic advice, Jack Hu and Mathias Renaud for immunostaining advice, and Stephen Banse, Eric Haig and the Cutter and Claycomb labs for their helpful discussion.

Funding: This research was supported by a Natural Sciences and Engineering Research Council of Canada (NSERC) Banting Postdoctoral Fellowship to KRK and NSERC Discovery Grant Program funding to ADC and LR. The funders had no role in study design, data collection and analysis, decision to publish, or preparation of the manuscript.

Author Contributions: KRK, ADC, and LR devised the project. KRK created strains VX194 and VX300. KRK performed the fecundity assay and experimental evolution. CR performed the immunostaining assays with assistance from KRK. KRK analyzed the data. KRK wrote the manuscript with the support of the other authors.

Data accessibility

The oligonucleotides used in this study are available as Table S1. The fertility data are available in File S1. The raw amplicon data will be made publicly available at NCBI SRA upon publication. The processed amplicon reads are available in File S2. The immunostaining data are available in File S3 and the complete protocol is available in File S4. All scripts are available via the Cutter Lab GitHub repository NSPF (https://github.com/Cutterlab/NSPF). Worm strains JK574 and VX300 are available from the *Caenorhabditis* Genetics Center. Strains PX814 and VX194 are available from the Cutter lab upon request.

References

Albritton, S.E., Kranz, A.-L., Rao, P., Kramer, M., Dieterich, C. & Ercan, S. (2014) Sex-biased gene expression and evolution of the x chromosome in nematodes. *Genetics*, **197**, 865–883.

Arnqvist, G. & Rowe, L. (2005) *Sexual conflict*. Princeton University Press.

Baldi, C., Cho, S. & Ellis, R.E. (2009) Mutations in two independent pathways are sufficient to create hermaphroditic nematodes. *Science*, **326**, 1002–1005.

Barker, D.M. (1994) Copulatory plugs and paternity assurance in the nematode *Caenorhabditis elegans*. *Animal Behaviour*, **48**, 147–156.

Barrett, R.D.H. & Hoekstra, H.E. (2011) Molecular spandrels: tests of adaptation at the genetic level. *Nature Reviews Genetics*, **12**, 767–780.

498 Begun, D.J., Whitley, P., Todd, B.L., Waldrip-Dail, H.M. & Clark, A.G. (2000) Molecular
499 population genetics of male accessory gland proteins in *Drosophila*. *Genetics*, **156**, 1879–
500 1888.
501 Brenner, S. (1974) The genetics of *Caenorhabditis elegans*. *Genetics*, **77**, 71–94.
502 Chapman, T. (2011) Seminal fluid-mediated fitness traits in *Drosophila*. *Heredity*, **87**, 511–521.
503 Cirera, S. & Aguade, M. (1997) Evolutionary history of the sex-peptide (Acp70A) gene region in
504 *Drosophila melanogaster*. *Genetics*, **147**, 189–197.
505 Clark, N.L., Aagaard, J.E. & Swanson, W.J. (2006) Evolution of reproductive proteins from
506 animals and plants. *Reproduction*, **131**, 11–22.
507 Dickinson, D.J., Pani, A.M., Heppert, J.K., Higgins, C.D. & 2015. (2015) Streamlined genome
508 engineering with a self-excising drug selection cassette. *Genetics*, **200**, 1035–1049.
509 Ellis, R.E. & Stanfield, G.M. (2014) The regulation of spermatogenesis and sperm function in
510 nematodes. *Seminars in Cell and Developmental Biology*, **29**, 17–30.
511 Gao, B. & Zhu, S. (2016) The drosomycin multigene family: three-disulfide variants from
512 *Drosophila takahashii* possess antibacterial activity. *Nature Reviews Genetics*, **6**, 32175.
513 Gray, J.C. & Cutter, A.D. (2014) Mainstreaming *Caenorhabditis elegans* in experimental
514 evolution. *Proceedings of the Royal Society B: Biological Sciences*, **281**, 20133055.
515 Hansen, J.M., Chavez, D.R. & Stanfield, G.M. (2015) COMP-1 promotes competitive advantage
516 of nematode sperm. *eLife*, 4:e05423.
517 Harris, T.W., Arnaboldi, V., Cain, S., Chan, J., Chen, W.J., Cho, J., *et al.* (2019) WormBase: a
518 modern model organism information resource. *Nucleic Acids Research*, **29**, 82.
519 Hirsh, D., Oppenheim, D. & Klass, M. (1976) Development of the reproductive system of
520 *Caenorhabditis elegans*. *Developmental Biology*, **49**, 200–219.
521 Hopkins, B.R. & Perry, J.C. (2022) The evolution of sex peptide: sexual conflict, cooperation,
522 and coevolution. *Biological Reviews*, **97**, 1426–1448.
523 Huan, Y., Kong, Q., Mou, H. & Yi, H. (2020) Antimicrobial peptides: classification, design,
524 application and research progress in multiple fields. *Frontiers in Microbiology*, **11**, 582779.
525 Kasimatis, K.R., Moerdyk-Schauwecker, M.J., Timmermeyer, N. & Phillips, P.C. (2018)
526 Proteomic and evolutionary analyses of sperm activation identify uncharacterized genes in
527 *Caenorhabditis* nematodes. *BMC Genomics*, **19**, 593.

528 Kenyon, C., Chang, J., Gensch, E., Rudner, A. & Tabtiang, R. (1993) A *C. elegans* mutant that
529 lives twice as long as wild type. *Nature*, **366**, 461–464.
530 Kleemann, G.A. & Basolo, A.L. (2007) Facultative decrease in mating resistance in
531 hermaphroditic *Caenorhabditis elegans* with self-sperm depletion. *Animal Behaviour*, **74**,
532 1339–1347.
533 Kruse, F., Junker, J.P., Oudenaarden, A. van & Bakkers, J. (2016) Tomo-seq: A method to obtain
534 genome-wide expression data with spatial resolution. *Methods in cell biology*, **135**, 299–307.
535 Lewontin, R.C. (1974) *The genetic basis of evolutionary change*. Columbia University Press.
536 McDonough, C.E., Whittington, E., Pitnick, S. & Dorus, S. (2016) Proteomics of reproductive
537 systems: Towards a molecular understanding of postmating, prezygotic reproductive barriers.
538 *Journal of Proteomics*, **135**, 26–37.
539 McGraw, L.A., Suarez, S.S. & Wolfner, M.F. (2015) On a matter of seminal importance.
540 *BioEssays*, **37**, 142–147.
541 Muir, R.E. & Tan, M.-W. (2008) Virulence of *Leucobacter chromiireducens* subsp. *solipictus* to
542 *Caenorhabditis elegans*: characterization of a novel host-pathogen interaction. *Applied and*
543 *Environmental Microbiology*, **74**, 4185–4198.
544 Nikonorova, I.A., Wang, J., Cope, A.L., Tilton, P.E., Power, K.M., Walsh, J.D., *et al.* (2022)
545 Isolation, profiling, and tracking of extracellular vesicle cargo in *Caenorhabditis elegans*.
546 *Current Biology*, **32**, 1–13.
547 Perry, J.C., Sirot, L. & Wigby, S. (2013) The seminal symphony: how to compose an ejaculate.
548 *Trends in Ecology & Evolution*, **28**, 414–422.
549 Poiani, A. (2006) Complexity of seminal fluid: a review. *Behavioral Ecology and Sociobiology*,
550 **60**, 289–310.
551 Rogers, A.B., Cormier, K.S. & Fox, J.G. (2006) Thiol-reactive compounds prevent nonspecific
552 antibody binding in immunohistochemistry. *Laboratory Investigation*, **86**, 526–533.
553 Samakovlis, C., Kylsten, P., Kimbrell, D.A., Engström, A. & Hultmark, D. (1991) The andropin
554 gene and its product, a male-specific antibacterial peptide in *Drosophila melanogaster*. *The*
555 *EMBO Journal*, **10**, 163–169.
556 Schärer, L., Janicke, T. & Ramm, S.A. (2015) Sexual conflict in hermaphrodites. *Cold Spring*
557 *Harbor Perspectives in Biology*, **7**, a017673.

558 Shakes, D.C., Wu, J., Sadler, P.L., LaPrade, K., Moore, L.L., Noritake, A., *et al.* (2009)
559 Spermatogenesis-specific features of the meiotic program in *Caenorhabditis elegans*. *PLoS*
560 *Genetics*, **5**, e1000611.
561 Sirot, L.K., Wong, A., Chapman, T. & Wolfner, M.F. (2015) Sexual conflict and seminal fluid
562 proteins: a dynamic landscape of sexual interactions. *Cold Spring Harbor Perspectives in*
563 *Biology*, **7**, a017533.
564 Smith, J.R. & Stanfield, G.M. (2011) TRY-5 Is a sperm-activating protease in *Caenorhabditis*
565 *elegans* seminal fluid. *PLoS Genetics*, **7,** e1002375.
566 Swanson, W.J. & Vacquier, V.D. (2002) Reproductive protein evolution. *Annual Review of*
567 *Ecology and Systematics*, **33**, 161–179.
568 R Core Team. (2020) *R: A language and environment for statistical computing*. Foundation for
569 Statistical Computing.
570 Teotonio, H., Estes, S., Phillips, P.C. & Baer, C.F. (2017) Experimental evolution with
571 *Caenorhabditis* nematodes. *Genetics*, **206**, 691–716.
572 Ting, J.J., Woodruff, G.C., Leung, G., Shin, N.-R., Cutter, A.D. & Haag, E.S. (2014) Intense
573 sperm-mediated sexual conflict promotes reproductive isolation in *Caenorhabditis*
574 nematodes. *PLoS Biology*, **12**, e1001915.
575 Wilburn, D.B. & Swanson, W.J. (2016) From molecules to mating: Rapid evolution and
576 biochemical studies of reproductive proteins. *Journal of Proteomics*, **135**, 12–25.
577 Wong, A. & Rundle, H. (2013) Selection on the *Drosophila* seminal fluid protein Acp62F.
578 *Ecology and Evolution*, **3**, 1942–1950.
579 Yin, D., Schwarz, E.M., Thomas, C.G., Felde, R.L., Korf, I.F., Cutter, A.D., *et al.* (2018) Rapid
580 genome shrinkage in a self-fertile nematode reveals sperm competition proteins. *Science*,
581 **359**, 55–61.
582

583 **Figures**

584

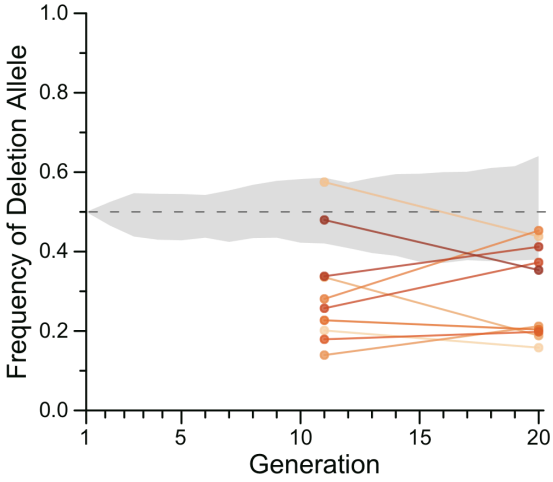

585

586 **Figure 1. Changes in the frequency of the deletion allele over time estimated using**
587 **amplicon sequencing data.** All ten replicates started with 50% deletion allele (dashed line). The
588 shaded gray region represents the expected allele frequency range under genetic drift and random
589 mating estimated by simulation. There was a significant decrease in the frequency of the deletion
590 allele over time (Model 1: $s = 0.001$, z-value = 3.3, $p < 0.001$; Model 2: $s = 0.0008$, z-value =
591 2.3, $p < 0.05$).

592

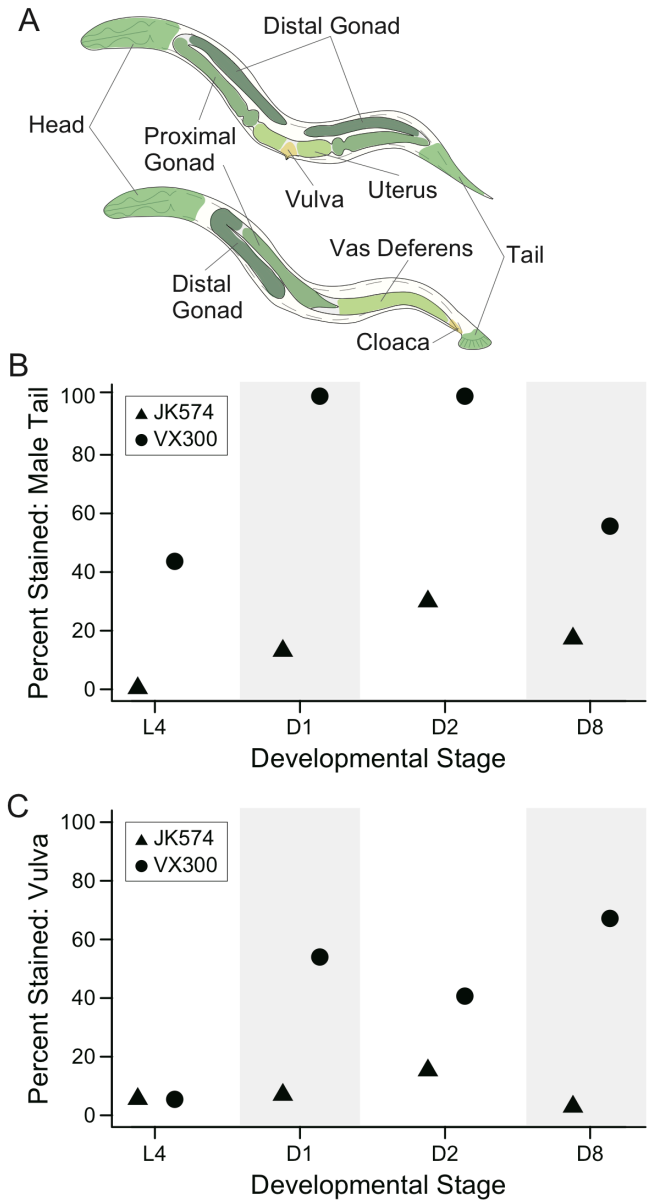

Figure 2. Quantification of antibody staining of 6x His-tagged NSPF-1. A) Diagram of the anatomical regions scored for presence of fluorescence in hermaphrodites/females and males. **B)** The percent of control males (JK574, triangle) and His-tagged males (VX300, circle) with fluorescence in the tail region during larval stage 4 (L4), day 1 of adulthood (D1), day 2 of adulthood (D2), and day 8 of adulthood (D8). **C)** The percent of control females (JK574, triangle) and His-tagged hermaphrodites (VX300, circle) with fluorescence in the vulva region during larval stage 4 (L4), day 1 of adulthood (D1), day 2 of adulthood (D2), and day 8 of adulthood (D8). Immunostaining counts across all anatomical regions is shown in Fig. S2.

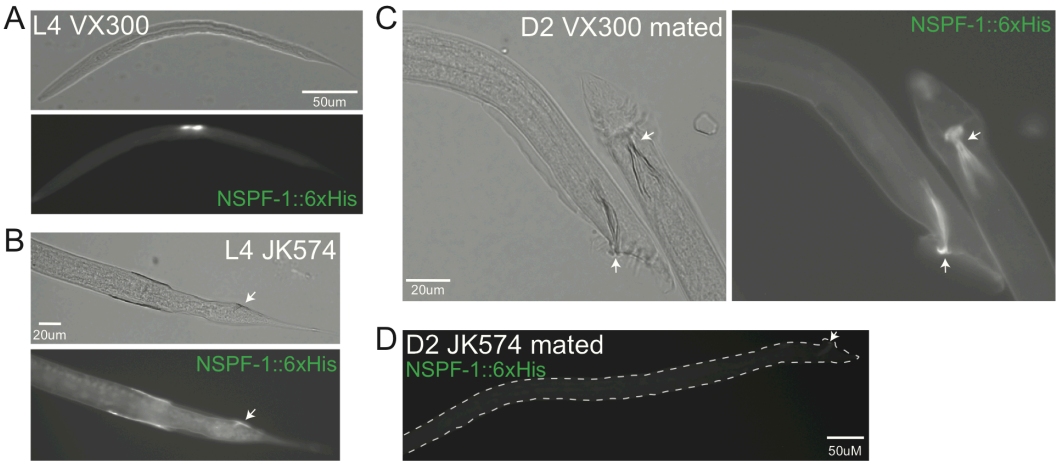

Figure 3. NSPF-1 localizes the spicules of adult males. A) Protein localized to the gonad of L4 His-tagged males. **B)** L4 control males showed off-target staining, especially in the cuticle, but not in the spicules. **C)** In adult His-tagged males, protein localized to the spicule structure in the male tail region. **D)** In adult control males, low levels of autofluorescence are detected in the spicules. However, the signal is markedly different than see in His-tagged males. In all images, the arrow points to the spicule.

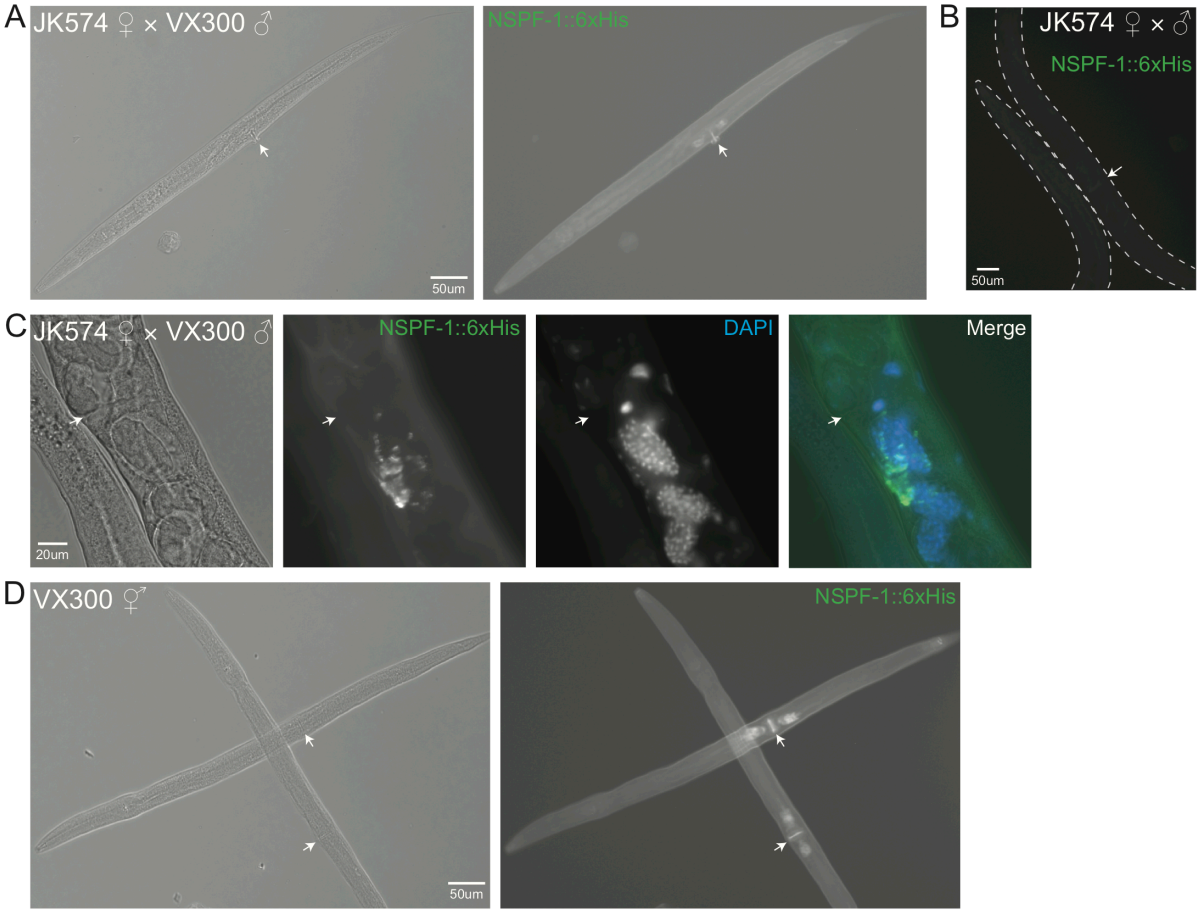

611

612 **Figure 4. NSPF-1 localizes to the vulva and uterus of mated females and adult**
613 **hermaphrodites. A)** Control pseudo-females mated to His-tagged males showed evidence of
614 protein localization in the vulva and uterus, especially when eggs were not yet present in the
615 uterus. **B)** Control pseudo-females mated to control males showed no evidence of staining. **C)**
616 Control pseudo-females mated with eggs present in the uterus after mating with His-tagged
617 males also had protein present in the uterus, though the signal was not always clear. However,
618 when present the proteins seemed to localize to the lumen and potentially along the surface of
619 vulva muscle cells, as shown in the merged image. **C)** His-tagged adult hermaphrodites who had
620 never been mated by a male showed the same protein localization in the uterus. In all images, the
621 arrow points to the vulva.

622 **Supplemental Files**

623 **Fig S1. Single male fecundity assays. A)** The total fecundity of wildtype males with the NSPF
624 genes (gray) and deletion males with the NSPF genes removed (orange) at day 1 of adulthood
625 and day 5 of adulthood. There was no significant difference in reproductive success between
626 male types. Day 1 data were replotted from Kasimatis et al. (2018). **B)** The proportion of
627 progeny coming from wildtype males (gray) or deletion males (orange) versus a wildtype
628 competitor male. There was no significant difference in sperm competitive ability between male
629 types (Kasimatis *et al.*, 2018). Competitive fecundity success data were replotted from Kasimatis
630 et al. (2018).

631

632 **Fig S2. Immunostaining quantification development. A)** Count data showing the percent of
633 control males (JK574, triangle) and His-tagged males (VX300, circle) with fluorescence in each
634 anatomical region during larval stage 4 (L4, orange), day 1 of adulthood (D1, green), day 2 of
635 adulthood (D2, blue), and day 8 of adulthood (D8, pink). **C)** Count data showing the percent of
636 control females (JK574, triangle) and His-tagged hermaphrodites (VX300, circle) with
637 fluorescence in each anatomical region during larval stage 4 (L4, orange), day 1 of adulthood
638 (D1, green), day 2 of adulthood (D2, blue), and day 8 of adulthood (D8, pink).

639

640 **Fig S3. NSPF-1 localizes the MOs of spermatids in adult males. A)** Protein (green) localized
641 in a punctate pattern around the nucleus (blue) of spermatids in the dissected testes of adult His-
642 tagged males. **B)** Protein localization within a single spermatid (outlined) of an adult His-tagged
643 male. **C)** Protein localization within multiple spermatids (arrows) of an adult His-tagged male.

644

645 **Table S1. Primers used in this study.**

646 **Table S2. Strains used in this study.**

647

648 **File S1. Late life fecundity data.**

649 **File S2. Processed amplicon reads.**

650 **File S3. Complete immunostaining protocols and buffer recipes.**

651 **File S4. Immunostaining data.**

652